Electronic Supplementary Material (ESI) for ChemComm.

Supporting Information

for

Dual effect of thiol addition on fluorescent polymeric micelles: ON-to-OFF switch and morphology transition

Anne B. Mabire [a], Mathew P. Robin [a], Helen Willcock [a], Anais Pitto-Barry [a], Nigel Kirby [b] and Rachel K. O'Reilly[a]*

[a] *Department of Chemistry, Library Road, University of Warwick, Coventry, CV4 7AL, UK. E-mail: r.k.o-reilly@warwick.ac.uk*

[b] *Australian Synchrotron, 800 Blackburn Road, Clayton, Victoria 3168, Australia*

I. Experimental

Materials and apparatus

Chemicals were used as received from Aldrich, Fluka and Acros. Dry solvents were obtained by passing over a column of activated alumina using an Innovative Technologies solvent purification system. TEGA was synthesized as previously reported and stored below 4 °C.[1] CTA, **1** and PLA_2, **1'**, were prepared as previously reported.[2, 3]

^1H and ^{13}C NMR spectra were recorded on a Bruker DPX-400 spectrometer in $CDCl_3$. Chemical shifts are given in ppm downfield from the internal standard tetramethylsilane (TMS). Size exclusion chromatography (SEC) measurements were conducted using a Varian 390-LC-Multi detector suite fitted with differential refractive index (DRI), light scattering (LS) and photodiode array (PDA) detectors equipped with a guard column (Varian Polymer Laboratories PLGel 5 μm, 50×7.5 mm) and two mixed D columns (Varian Polymer Laboratories PLGel 5 μm, 300×7.5 mm). The mobile phase was either tetrahydrofuran (THF) with 2% triethylamine (TEA) or dimethylformamide (DMF) with 5 mmol NH_4BF_4 at 50 ^oC operating at a flow rate of 1.0 mL·min^{-1} and data was analyzed using Cirrus v3.3 with calibration curves produced using Varian Polymer laboratories Easi-Vials linear poly(styrene) or poly(methyl)methacrylate standards. Multi-angle Laser Light Scattering measurements were performed at angles of observation ranging from 30° up to 150° with an ALV CGS3 setup operating at λ_0 = 632nm and at 25°C ± 1°C, the data was collected with 100s run time in duplicate unless otherwise specified. Calibration was achieved with filtered toluene and the background was measured with 18.2 MΩ.cm water. Electric field autocorrelation functions ($g_1(q,t)$) were fitted with CONTIN. Synchrotron small-angle X-ray scattering (SAXS) measurements were carried on the SAXS/WAXS beamline at the Australian Synchrotron facility at a photon energy of 11 keV. The samples in solution were run by using a 1.5 mm diameter quartz capillary. Temperature was held at 25 °C and controlled *via* a water bath connected to a brass block which is part of the sample holder. The measurements were collected at a sample to detector distance of 7.323 m to give a q range of 0.02 to 0.14 Å^{-1}, where q is the scattering vector and is related to the scattering angle (2θ) and the photon wavelength (λ) by the following equation:

$$q = \frac{4\pi \, sin(\theta)}{\lambda}$$

All patterns were normalised to fixed transmitted flux using a quantitative beamstop detector. The scattering from a blank was measured in the same capillary and was subtracted for each

measurement. The two-dimensional SAXS images were converted in one-dimensional SAXS profile (*I(q) versus q*) by circular averaging, where *I(q)* is the scattering intensity. The functions used for the fitting from the NIST SANS analysis package were "Guinier-Porod",[4, 5] "Debye",[6] "PolyCoreForm"[7] and "Debye".[6] ScatterBrain[8] and Igor[9] were used to plot and analyse the data. The scattering length density of the solvent and the monomers were calculated using the "Scattering Length Density Calculator"[10] provided by NIST Center for Neutron Research. Limits for *q* range were applied for the fittings from 0.002 to 0.1 $Å^{-1}$. Solutions of graphene oxide were synthesised as reported previously.[10a] Aqueous solutions of graphene oxide (0.10 mg mL^{-1}) were sonicated for 30 s prior to use. Lacey carbon grids (400 Mesh, Cu) (Agar Scientific) were cleaned using air plasma from a glow-discharge system (2 min, 20 mA). The TEM grids were placed on a filter paper and one drop (≈ 0.08 mL) of the sonicated GO solution was deposited onto each grid from a height of ≈ 1 cm, allowing the filter paper to absorb the excess solution, and the grids were left to air-dry in a dessicator cabinet for ≈ 60 min. 4 μL of the nanoparticle dispersion (~20 ppm) was pipetted onto a GO grid and left to air-dry in a dessicator cabinet for ≈ 60 min. Brightfield TEM images were captured with a transmission electron microscope (JEOL TEM-2011), operating at 200 kV. Fluorescence spectra were recorded using a Perkin-Elmer LS 55 Fluorescence Spectrometer.

Synthetic protocols

The block copolymer PTEGA-*b*-PLA_2, **2**, has been synthesised as previously reported.[3]

*Self-assembly of PTEGA-b-PLA_2 micelles, **3***

The self-assembly of copolymer, **2,** into micelles, **3,** was performed by direct dissolution of **2** in 18.2 MΩ.cm water at concentrations of 0.5 $mg.mL^{-1}$, 1 $mg.mL^{-1}$ and 2 $mg.mL^{-1}$.

Addition-Elimination reaction with PTEGA-b-PLA_2 micelles

20 equivalents of thiophenol were added to **3**. The reaction was stirred at room temperature for 1 h. The mixture was purified *via* exhaustive dialysis (MWCO = 1000 Da) against 18.2 MΩ.cm water to remove the excess thiophenol, centrifuged to separate the precipitate (**6**) and freeze-dried. The resultant solid was resuspended at 1 $mg.mL^{-1}$ to give a solution of vesicles (**4a**).

Addition-Elimination reaction with PTEGA homopolymer

Polymer **5** was dissolved in 18.2 MΩ.cm water at 1 mg/mL and 20 equivalents of thiophenol were added to the solution. The reaction was stirred at room temperature for 1 h. The mixture was purified *via* exhaustive dialysis (MWCO = 1000 Da) against 18.2 MΩ.cm water to remove the excess of thiophenol and freeze-dried. The resultant solid was resuspended at 1 $mg.mL^{-1}$ to give a solution of vesicles (**4b**).

II. Characterisation data

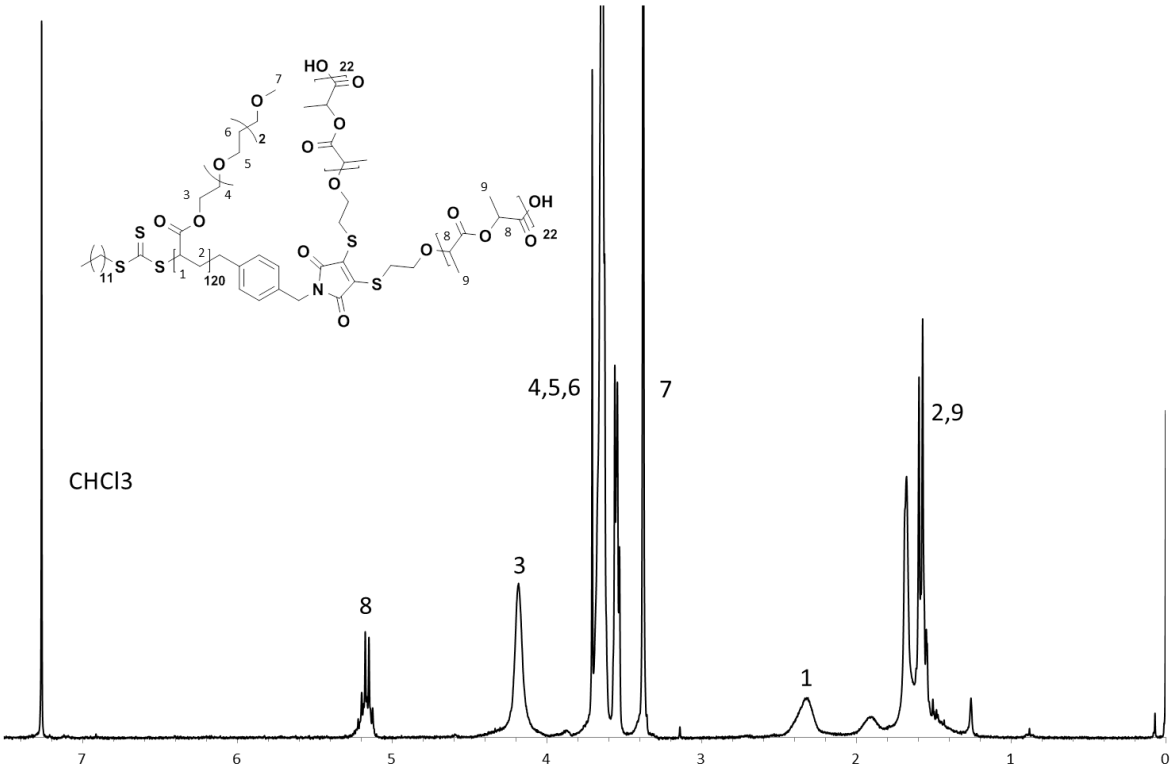

Figure S1. ^{1}H NMR (400 MHz, $CDCl_3$) spectrum of PTEGA-*b*-PLA_2, **2**.

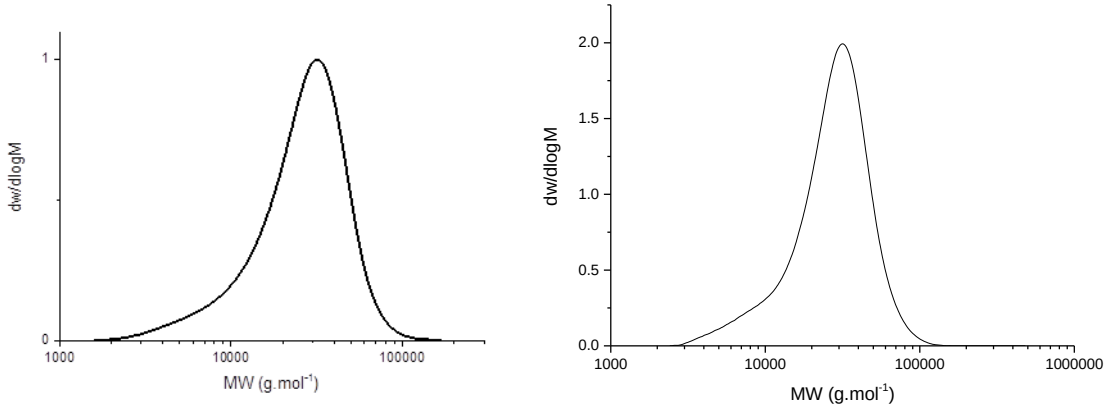

Figure S2. Molecular weight distribution obtained by SEC, LHS: using polystyrene calibration and THF as the eluent and RHS using polymethylmethacrylate calibration and DMF as the eluent for the block copolymer PTEGA-b-PLA2, **2**.

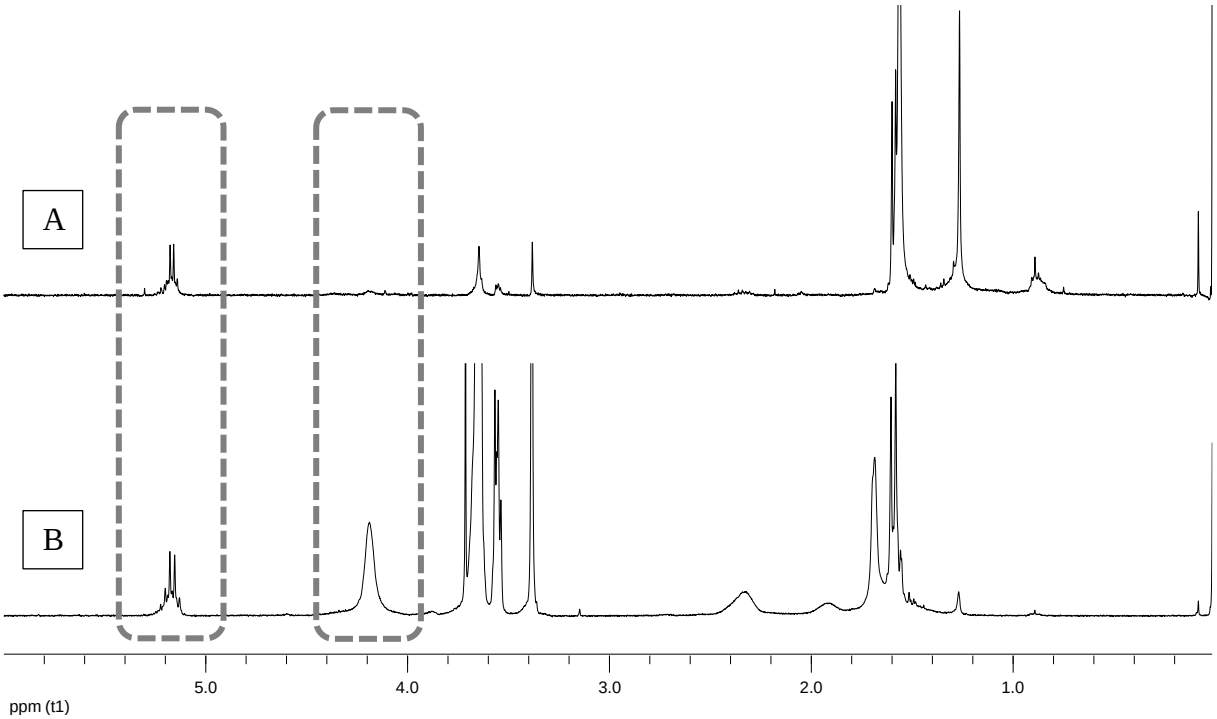

Figure S3. (A) ^{1}H NMR (400 MHz, $CDCl_3$) spectrum of the thio-PLA, **6**, obtained after separation following the addition-elimination reaction compared to (B) ^{1}H NMR (400 MHz, $CDCl_3$) spectrum of block copolymer PTEGA-*b*-PLA_2, **2** in $CDCl_3$. Highlighting the presence of the characteristic PLA signal at 5.2 ppm and the absence of characteristic TEGA signal at 4.2 ppm.

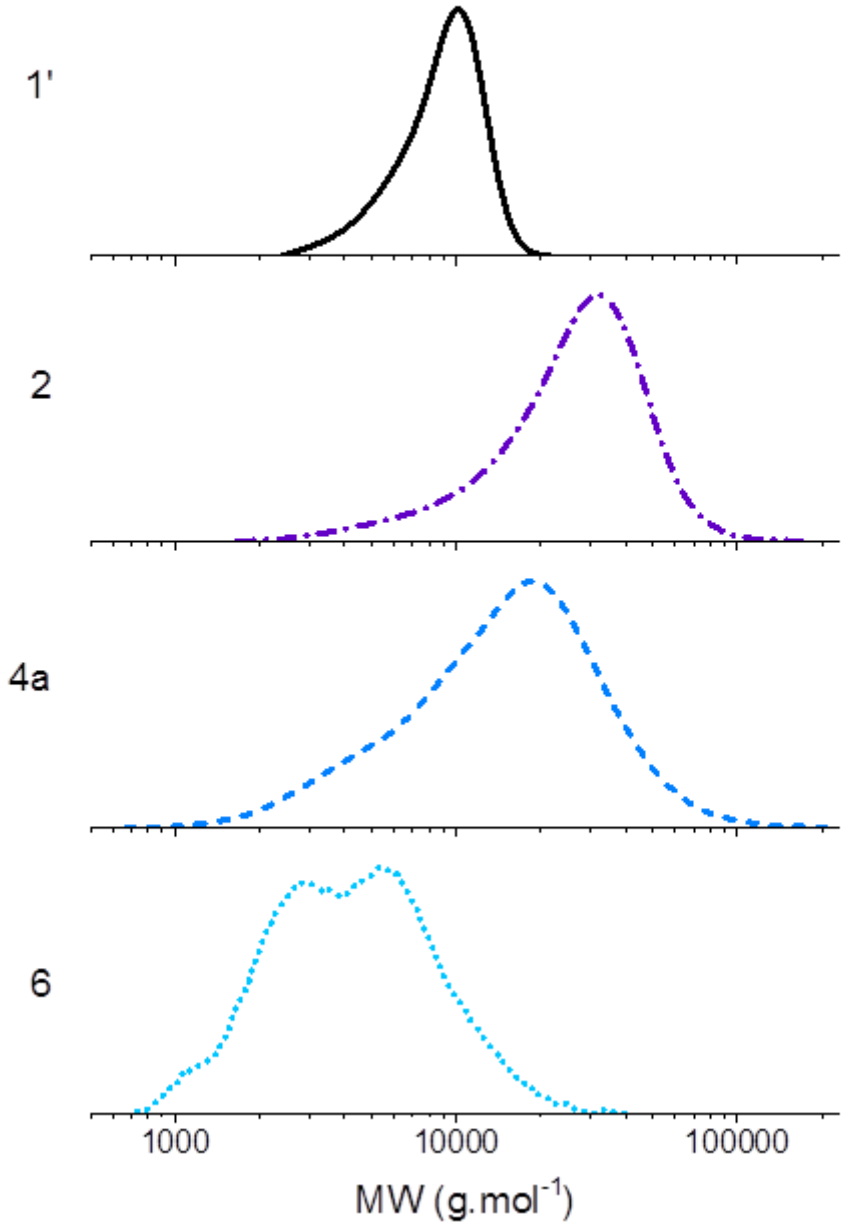

Figure S4. Molecular weight distribution obtained by SEC, using polystyrene calibration and THF as the eluent for the block copolymer precursor PLA_2 **(1')**, PTEGA-*b*-PLA_2 (**2**), purified product of the addition-elimination reaction (**4a**) with residual polylactide and the PLA precipitate (**6**).

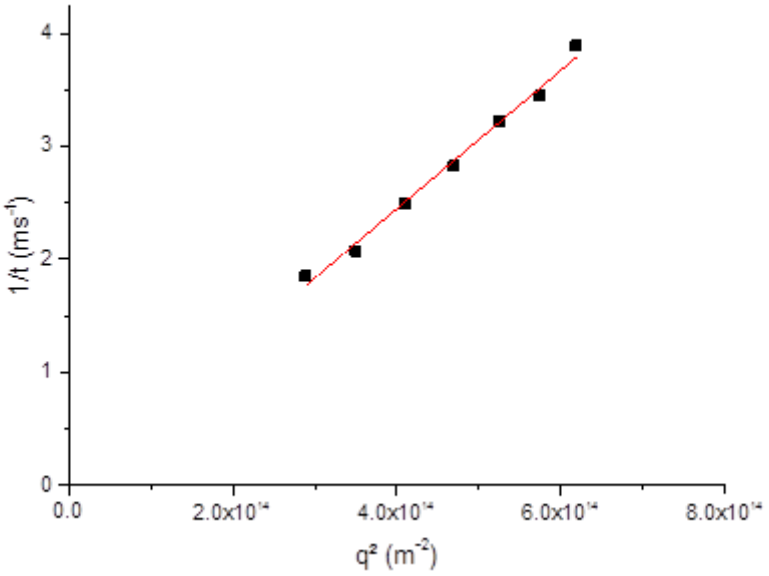

Figure S5. Plot of τ-1 vs. q^2 for micelles (1 mg.mL^{-1}), **3**.

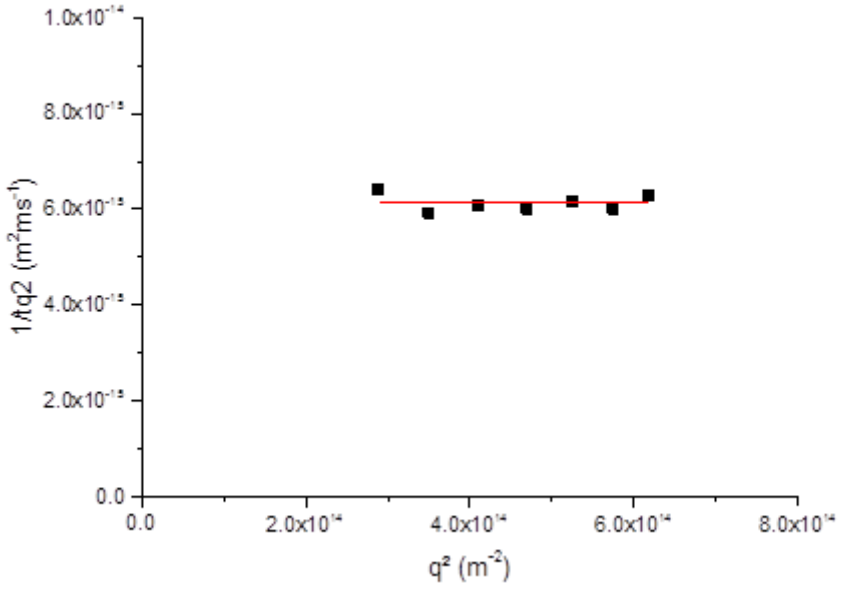

Figure S6. Plot of $\tau^{-1}q^{-2}$ *vs.* q^2 for micelles (1 mg.mL^{-1}), **3**.

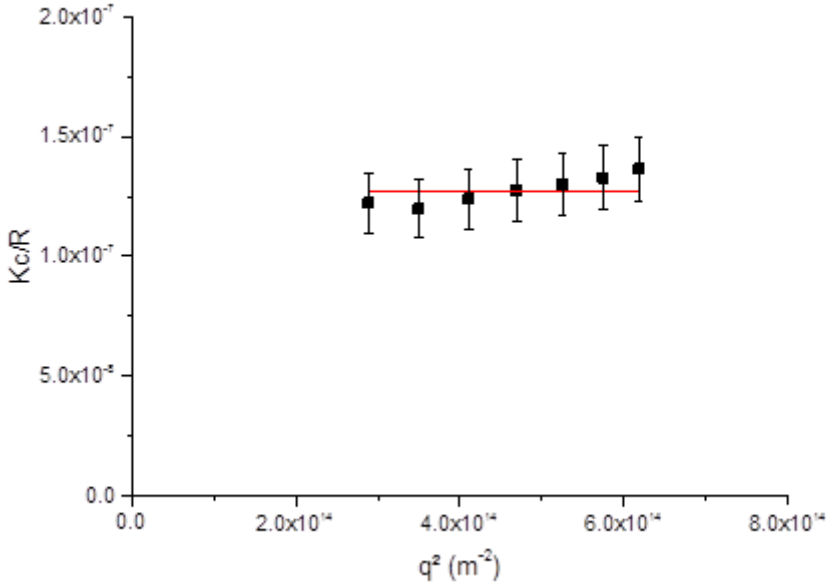

Figure S7. Plot of Kc/R *vs.* q^2 for micelles (1 mg.mL^{-1}), **3**.

Note for particles smaller than λ/20, only a negligible phase difference exists between light emitted from the various scattering centers within the given particle. In this case, the detected scattered intensity will be independent of the scattering angle and only depend on the mass of the particle which is proportional to the total number of scattering centers one particle contains.[11]

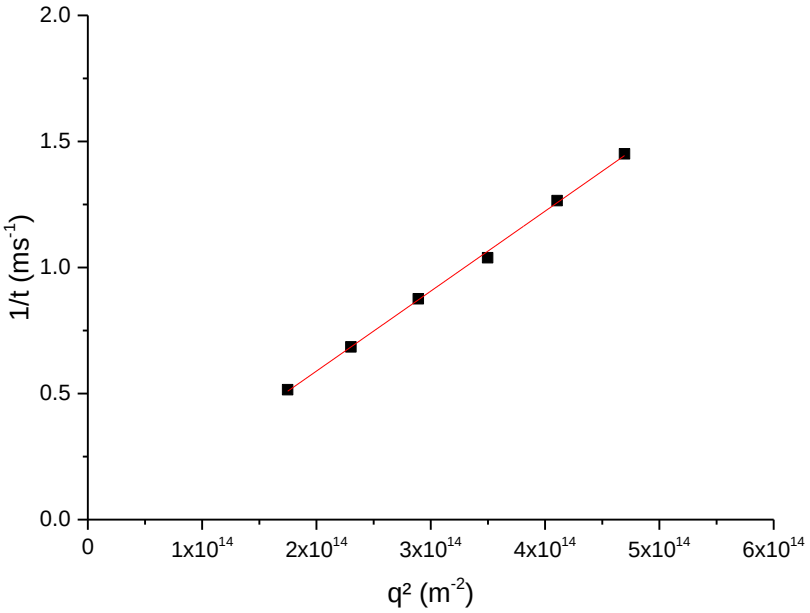

Figure S8. Plot of τ^{-1} *vs.* q^2 for the product, **4a** (2 mg.mL^{-1}), of the reaction of thiophenol with micelles, **3,** prior to centrifugation, drying and re-suspension.

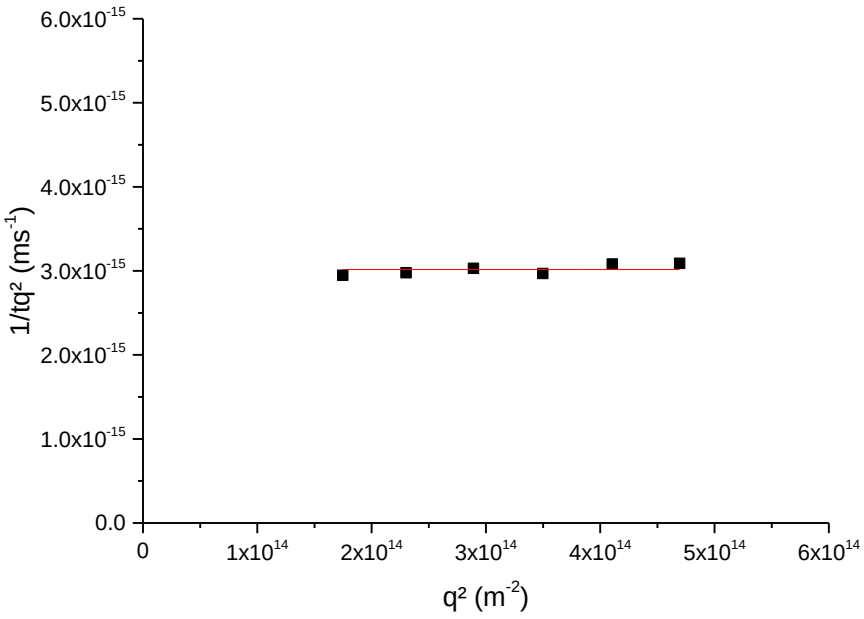

Figure S9. Plot of $\tau^{-1}q^{-2}$ *vs.* q^2 for the product, **4a** (2 mg.mL^{-1}), of the reaction of thiophenol with micelles, **3,** prior to centrifugation, drying and re-suspension.

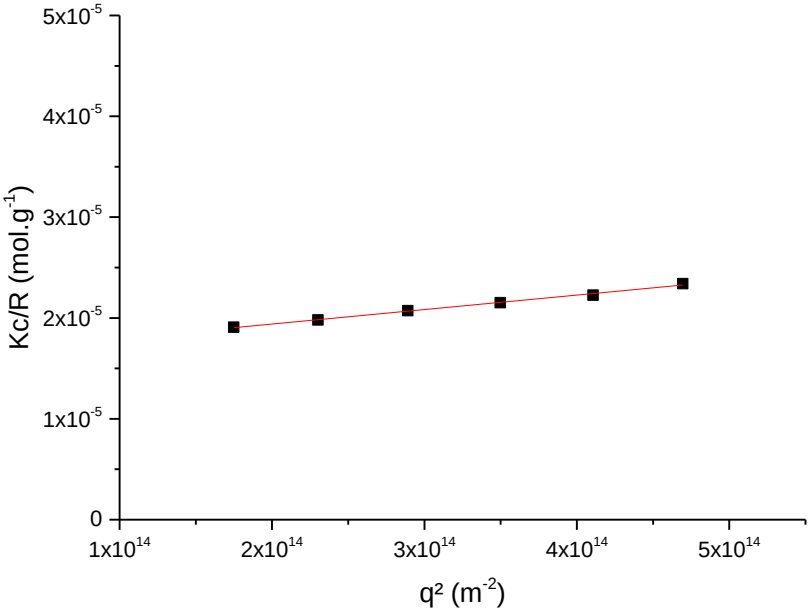

Figure S10. Plot of Kc/R *vs.* q² for the product, **4a** (2 mg.mL^{-1}), of the reaction of thiophenol with micelles, **3,** prior to centrifugation, drying and re-suspension.

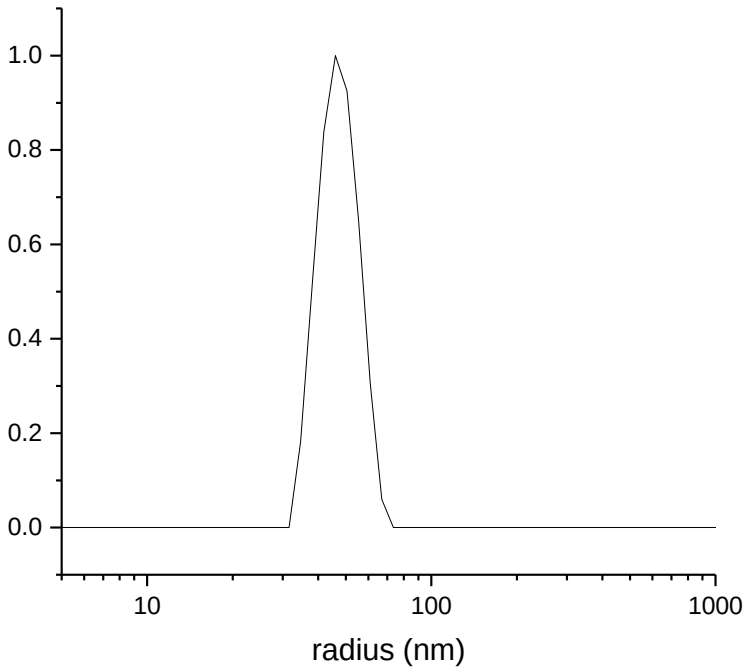

Figure S11. Size distribution for the nanostructure **4a** (2 mg.mL^{-1}) at 90°

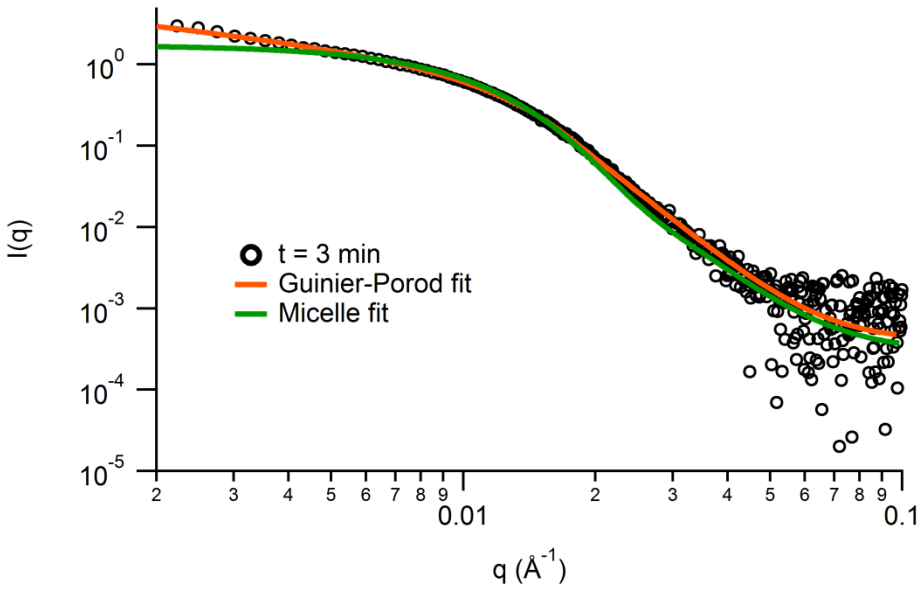

Figure S12. SAXS profile and fits for the reaction of **3** with thiophenol after 3 min. The Guinier-Porod fit gives a R_g value of 12 nm, such a difference with LS can be explained by the hydration of the PTEGA core, and thus the radius visible by SAXS corresponds to the radius of the core and a partial layer of the shell, the one which is more dense and near the core. Such an incomplete visibility of a hydrophilic corona has already been observed.[12, 13] The PolyCoreForm used for this fit is considered as a uniform micelle with some dispersity ($Đ$ = 0.3), a radius of 14 nm was obtained, which fits well with the R_g obtained with the Guinier-Porod plot. The scattering length density of the micelle was found slightly higher than usual for lactide, which suggests the incorporation of some PTEGA in this layer.

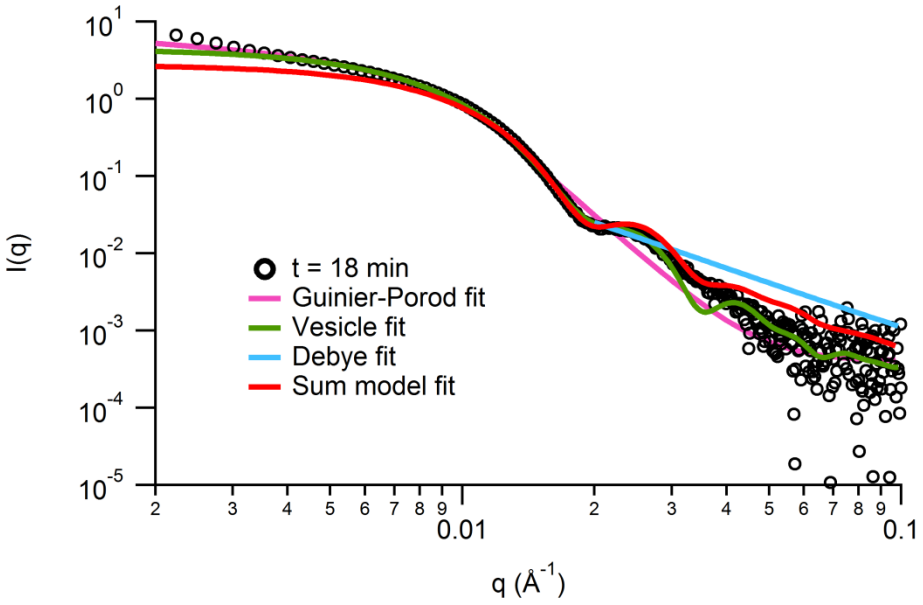

Figure S13. SAXS profile and fits for the reaction of **3** with thiophenol after 18 min. The Guinier-Porod fit gives a R_g value of 20 nm, which is lower than the value determined by LS. Again, the hydration of PTEGA does not allow for the polymer to be entirely visible by SAXS. A PolyCoreForm with a core-shell structure fit the experimental curvefor *q* values below 0.025 $Å^{-1}$, which suggests the presence of another morphology with poorly-defined form factor in the solution. This correlates well with the presence of polylactide in solution. Polylactide being hydrophobic, it tends to form collapsed coils in water, which was confirmed by a Debye fit. To further confirm the presence of these two structures in solution, a linear combination of the PolyCoreForm with a core-shell structure and Debye fits was performed. This Sum model confirms the structure of vesicles with a large dispersity on the core. These vesicles are seems as a core full of water with a radius of 4 nm and a shell of PTEGA with a thickness of 19 nm. These values are similar to the ones obtained with the PolyCoreForm fit for vesicle alone, and are in good agreement with the Guinier-Porod fit. The addition of random coil polymer allowed for a better fit for *q* values above 0.025 $Å^{-1}$.

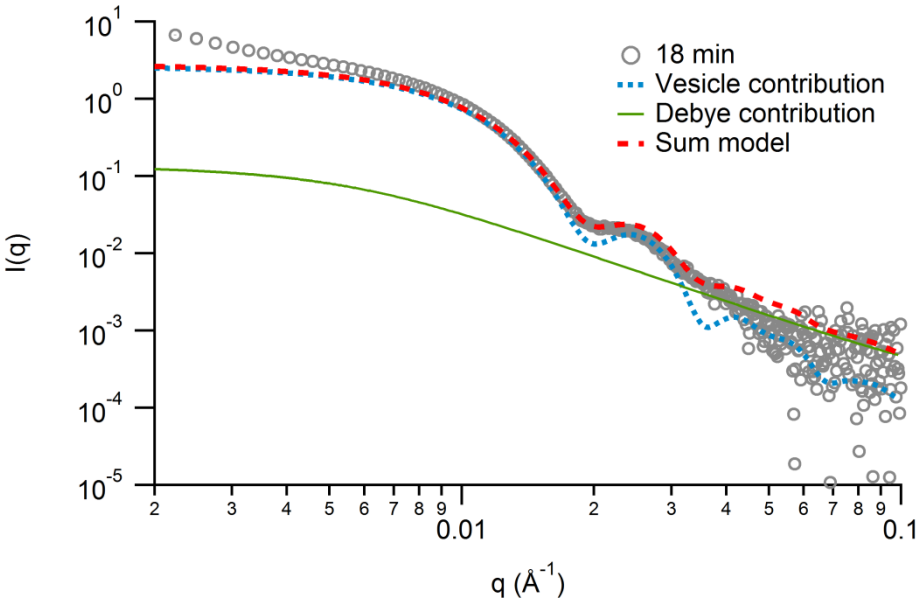

Figure S14. SAXS data after 18 minutes of reaction of **3** with thiophenol. The two components of the Sum model used previously are shown. The vesicle contribution is much more important at low q than the Debye one and for q above 0.015 Å, the two models contribute more equally.

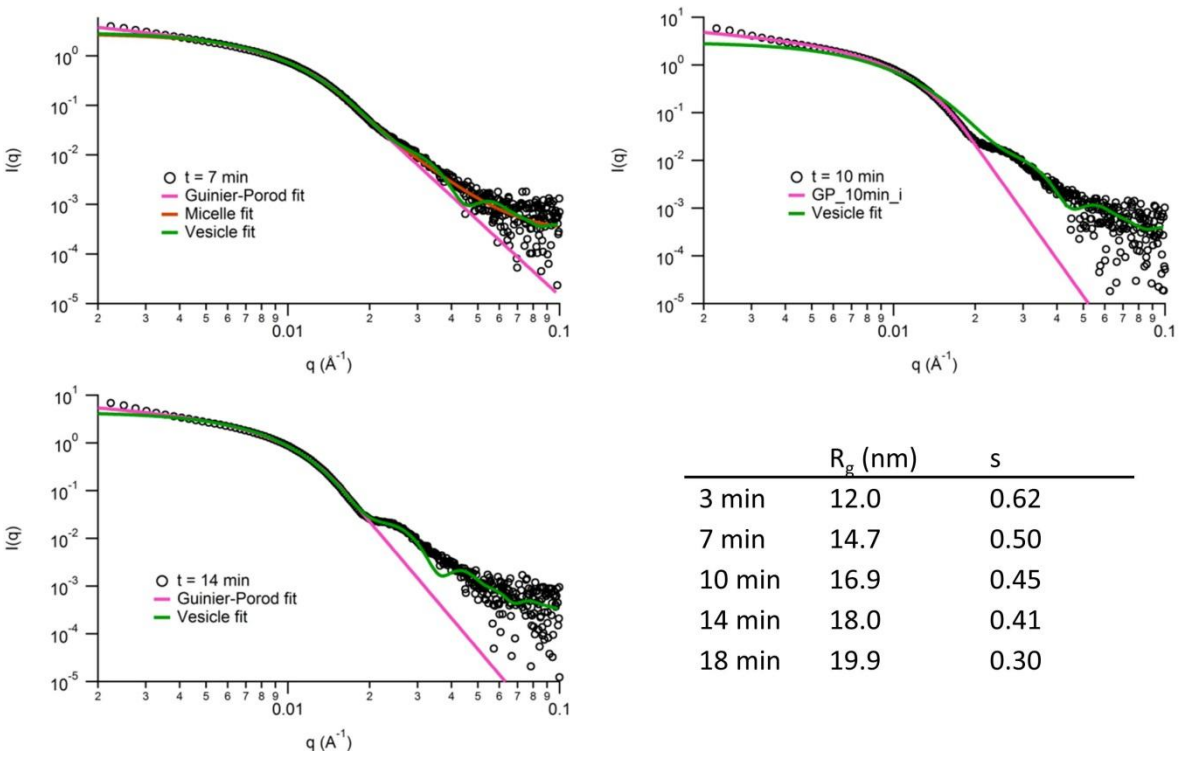

	R_g (nm)	s
3 min	12.0	0.62
7 min	14.7	0.50
10 min	16.9	0.45
14 min	18.0	0.41
18 min	19.9	0.30

Figure S15. SAXS curves and fits at different time point during the reaction of **3** with thiophenol. A Guinier-Porod used for each curve provides general information on the shape and size of the sample in solution (see values in Table). The values follow a trend: bigger particles are obtained after the reaction, and they are more spherical than at the beginning of the reaction. A transition from spherical micelle to vesicle is confirmed by the change of shape of the raw data curves and the poor fit provided by the micelle model after 7 min.

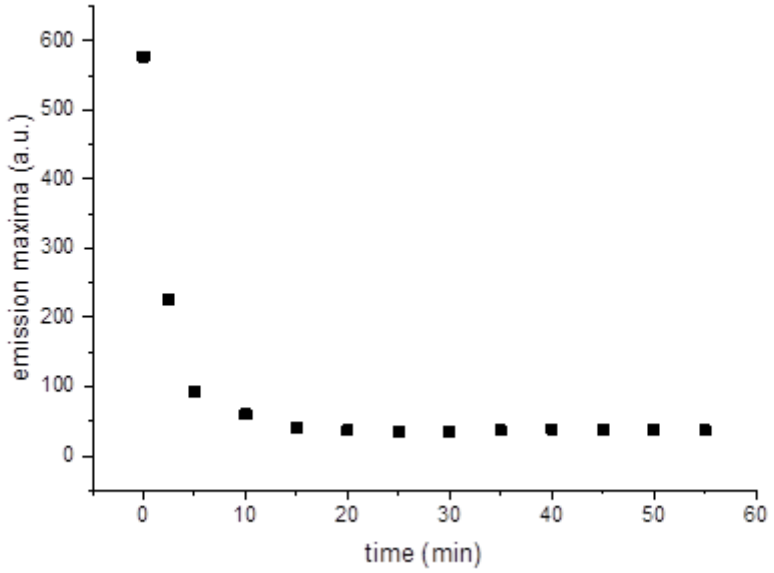

Figure S16. Variation of fluorescence emission maxima at 510 nm over time after addition of thiophenol to micelles, **3**. Excitation wavelength 405 nm.

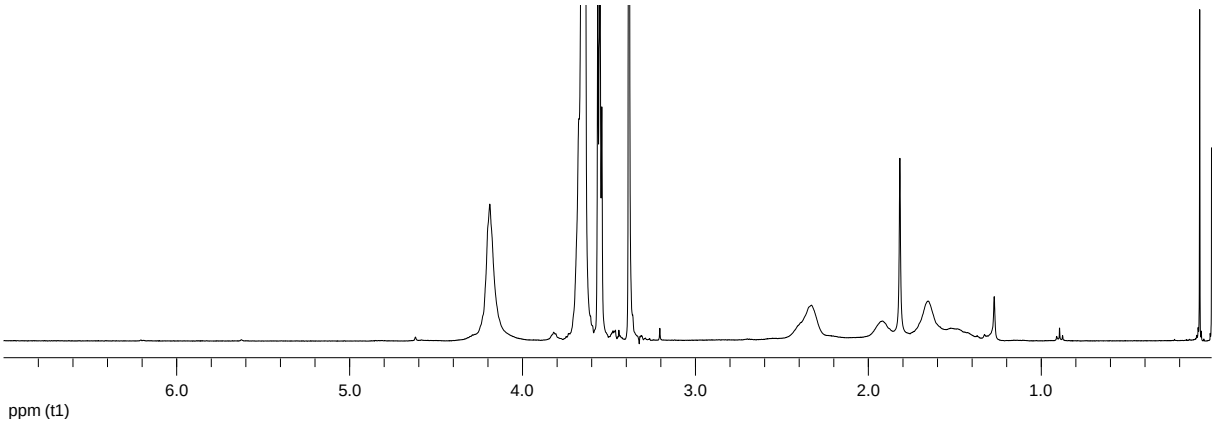

Figure S17. ^{1}H NMR (400 MHz, $CDCl_3$) spectrum of PTEGA, **5**.

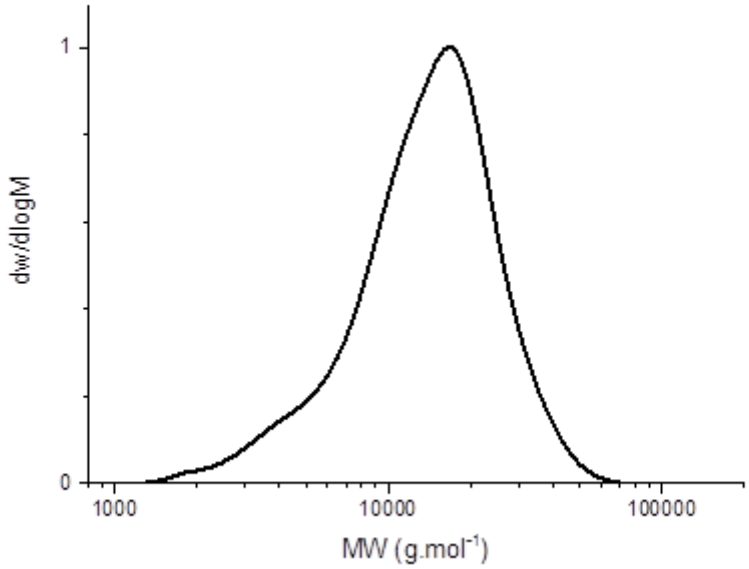

Figure S18. Molecular weight distribution obtained by SEC, using polystyrene calibration and THF as the eluent for the homopolymer PTEGA, **5**.

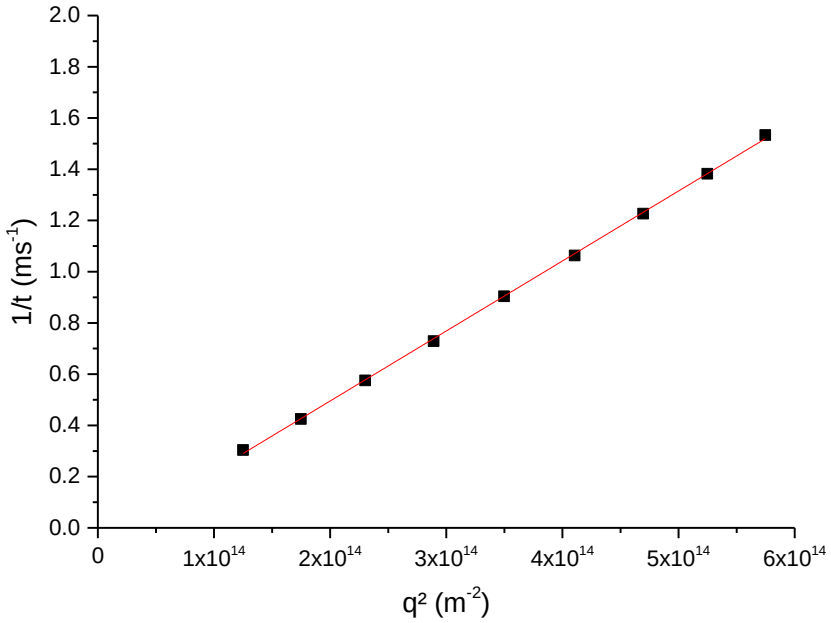

Figure S19. Plot of τ^{-1} *vs.* q^2 for the product, **4b** (2 mg.mL^{-1}), of the reaction of thiophenol with homopolymer, **5**.

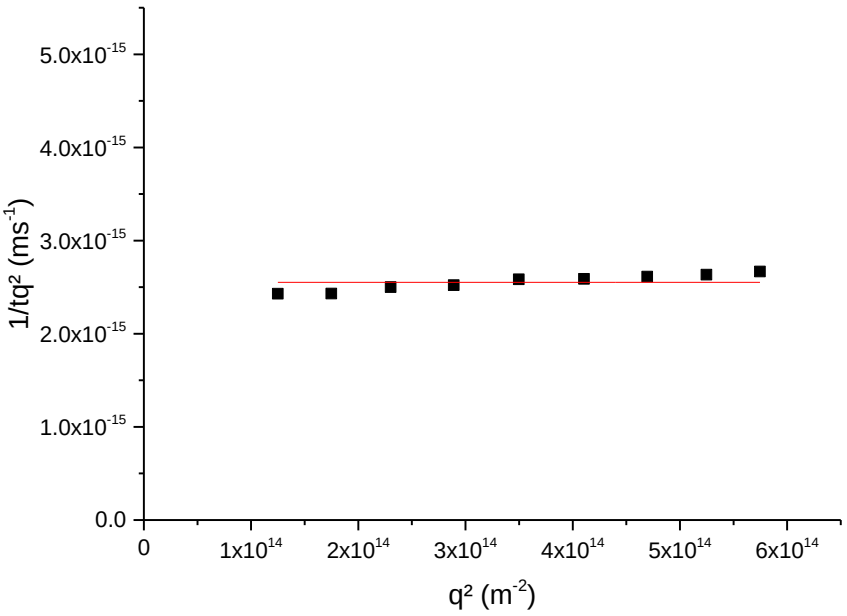

Figure S20. Plot of $\tau^{-1}q^{-2}$ *vs.* q^2 for the product, **4b** (2 mg.mL^{-1}), of the reaction of thiophenol with homopolymer, **5**.

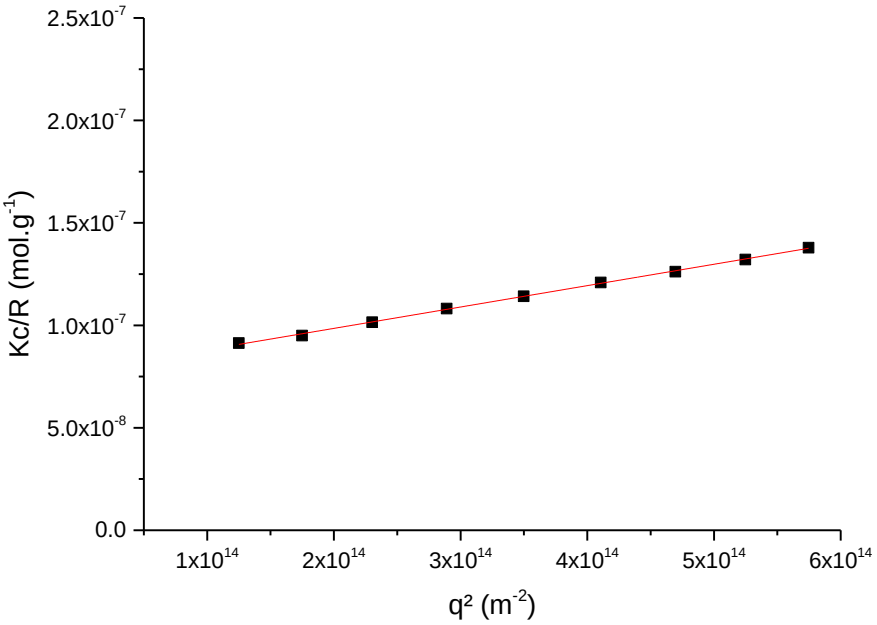

Figure S21. Plot of Kc/R *vs.* q² for the product, **4b** (2 mg.mL^{-1}), of the reaction of thiophenol with homopolymer, **5**.

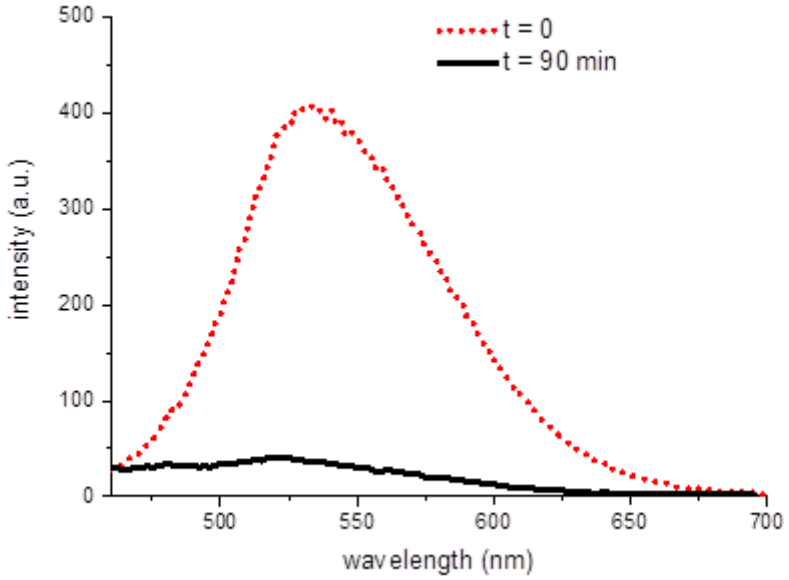

Figure S22. Fluorescence emission spectra for the addition-elimination reaction of homopolymer (**5**) with thiophenol, before the reaction (dotted line) and after the reaction (solid line) solution **4b**. Emission maxima at 535 nm with an excitation wavelength of 415 nm.

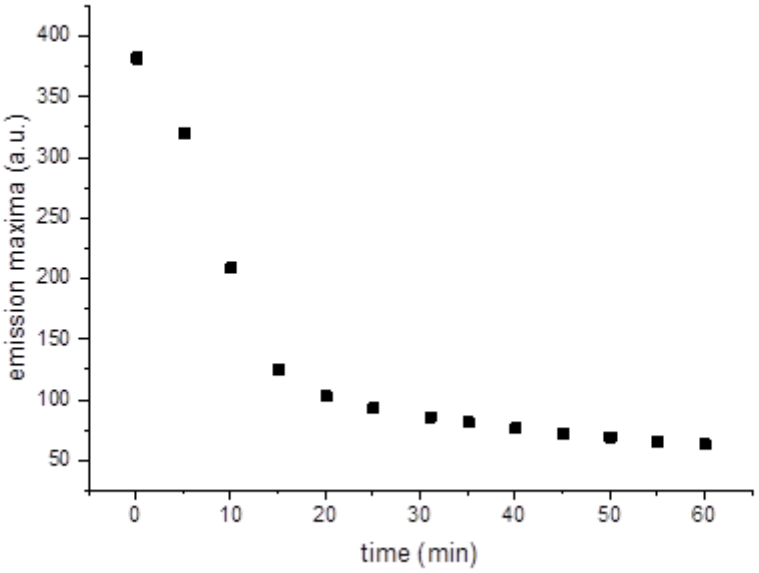

Figure S23. Variation of fluorescence emission maxima at 535 nm over time after addition of thiophenol to the homopolymer, **5**. Excitation wavelength 415 nm.

References

1. F. Hua, X. Jiang, D. Li and B. Zhao, *J Polym Sci, Part A: Polym Chem*, 2006, **44**, 2454-2467.
2. M. P. Robin, P. Wilson, A. B. Mabire, J. K. Kiviaho, J. E. Raymond, D. M. Haddleton and R. K. O'Reilly, *J Am Chem Soc*, 2013, **135**, 2875-2878.
3. M. P. Robin, A. B. Mabire, J. C. Damborsky, E. S. Thom, U. H. Winzer-Serhan, J. E. Raymond and R. K. O'Reilly, *J Am Chem Soc*, 2013, **135**, 9518-9524.
4. A. Guinier and G. Fournet, *Small-angle scattering of X-Rays*, John Wiley & Sons, New York, 1955.
5. O. Glatter and O. Kratky, *Small-Angle X-Ray Scattering*, Academic Press, 1982.
6. R.-J. Roe, *Methods of X-ray and Neutron Scattering in Polymer Science*, Oxford University Press, New York, 2000.
7. P. Bartlett and R. H. Ottewill, *J Chem Phys*, 1992, **96**, 3306-3318.
8. S. T. Mudie, *scatterBrain*, (2013), Australian Synchrotron.
9. S. Kline, *J Appl Crystallogr*, 2006, **39**, 895-900.
10. NIST SLD calculator.
11. J. P. Patterson, M. P. Robin, C. Chassenieux, O. Colombani and R. K. O'Reilly, *Chem Soc Rev*, 2014, **43**, 2412-2425.
12. A. Pitto-Barry, N. Kirby, A. P. Dove and R. K. O'Reilly, *Polym Chem*, 2014, **5**, 1427-1436.
13. L. Sun, N. Petzetakis, A. Pitto-Barry, T. L. Schiller, N. Kirby, D. J. Keddie, B. J. Boyd, R. K. O'Reilly and A. P. Dove, *Macromolecules*, 2013, **46**, 9074-9082.